conditions. Testing of this nature in a natural environment is cost prohibited. To conduct these tests, the military services use the U.S. Air Force Climatic Laboratory at Eglin AFB in Florida. In the climatic hangar, aircraft systems, subsystems, and components can be functionally operated at temperatures from −65 to +125°F. Tests are conducted on fully instrumented, operational aircraft. Provisions are provided in the hangar to run the engines and rotor systems through their full operating range. Approximately two months of testing is required to cover the entire temperature range.

Airworthiness and Flight Characteristic (A&FC)

The A&FC is conducted on a production prototype or production aircraft delivered from either an initial or a pilot production run after the milestone III decision has been made. The test determines whether or not the transition from an engineering development prototype to a production item has been made successfully and whether the system meets contract and military specifications. Specifically the tests determine:

1) Detailed information on performance, stability and control, powerplant operation, and integrated system characteristics.

2) Data for technical manuals.

3) Verification of the recommended flight envelope for operational use.

The scope of test varies from 80-150 flight hours. Performance tests include six-to-eight level flight speed power polars, forward flight climb, autorotational descent, hover, takeoff and landing, vertical climb, and height-velocity. Flying qualities tests include control positions, static longitudinal stability, static lateral-directional stability, maneuvering stability, control response, dynamic stability, and degraded modes. Operational-type tests such as slope landings, mission maneuvers, and instrument/night flight may also be included. All these tests are conducted at several center of gravity positions and density altitudes.

The A&FC is the last formal development test in the acquisition cycle. Engineering change proposals may require development testing during the production/deployment phase.

Operational Testing

Operational testing (OT) is done by an organization that is independent of the developing, procuring, and using commands. The tests are accomplished with typical user operators, crews, or units in as realistic an operational environment as possible. The purpose of OT is to determine the effectiveness and suitability of the system in a simulated combat situation. The adequacy of doctrine, organization, operating techniques, tactics, and training are also evaluated.

Operational Test I

OTI is conducted during the validation phase and should provide an indication of military utility and worth to the user.

Operational Test II

OTII is done prior to the milestone III production decision. The purpose is the same as previously discussed. The scope of tests may involve several prototype aircraft which may be flown against a type or model aircraft for comparison. Unlike the developmental testing, trained testers and sterile test environments are not used. As pointed out in the introduction, considerable emphasis has been placed on the results of these tests. A technically superior weapon system which has been successfully evaluated in developmental testing may be shown to be unsuitable in the real world.

Conclusion

The information gained from successful accomplishment of the developmental, operational, and environmental tests is a key requirement for decisions to commit additional resources to a program or to advance it from one acquisition phase to another. It is the objective of the government tests to field a defense weapon system that is technically proved, operationally effective, and meets the threat.

AIAA 82-4154

Incompressible Symmetric Flow Characteristics of Sharp-Edged Rectangular Wings

Erik S. Larson*
The Aeronautical Research Institute of Sweden, FFA Stockholm, Sweden

Nomenclature

A	= aspect ratio
c	= wing chord
c.g.	= center of gravity, reference point, 0.25 chord
c.p.	= center of pressure
ΔC_D	$= C_D - C_{D_0}$ = lift-dependent drag/qS, lift-dependent drag coefficient
C_L	= lift/qS, lift coefficient
C_m	= pitching-moment/qSc, pitching moment coefficient
C_N	= normal force/qS, normal force coefficient
F_1, F_2, F_3	= empirical correction factors
K_p	$= \partial(C_{N,p})/\partial(\sin\alpha\cos\alpha)$
$K_{v,\text{le}}$	= ∂(2 leading-edge suction force from one side/qS)/$\partial\sin^2\alpha$
$K_{v,\text{se}}$	= ∂(2 tip suction force from one side edge/qS)/$\partial\sin^2\alpha$
$\bar{K}_{v,\text{se}}$	= ∂(2 tip suction force from one side edge/qS)/$\partial\sin^{5/3}\alpha$
M	= Mach number
q	= freestream dynamic pressure
S	= wing area
x	= streamwise coordinate, origin at the leading edge
α	= angle of attack, deg
β	$= \sqrt{1-M^2}$
ξ	$= (x_{\text{ref}} - x_l)/c$, dimensionless distance between reference point and c.p. of the aerodynamic item in question

Subscripts

p	= potential or attached flow
v, le	= vortex effect at the leading edge
v, se	= vortex effect at the side edge

Introduction

In a previous Note,[1] the symmetric, aerodynamic characteristics—lift, lift-dependent drag, and pitching moment coefficients—on sharp-edged rectangular wings were obtained by a set of semiempirical, analytical formulas that

Received Nov. 17, 1981; revision received Jan. 15, 1982.

*Senior Research Engineer, Department of Aerodynamics. Member AIAA.

represented Lamar's extension of the Multhopp solution.[2] A difference between theory and experiment has been noticed, however, in regard to the lift and pitching moment coefficients for all of the investigated aspect ratios except $A=1$.

This Note investigates whether this discrepancy is a result of the formulation of the angle of attack squared (α^2) in combination with the side-edge suction force coefficient, i.e., $K_{v,se}\sin^2\alpha$, in Polhamus'[3] and Lamar's[2] nomenclature. Several theoretical works indicate that an exponent of 5/3 would be more correct. Kaden[4] (rollup of a discontinuity surface); Legendre,[5] Adams,[6] and others (delta wings); and Cheng[7] (rectangular wings) all arrive at the same exponent of 5/3 (i.e., $\alpha^{5/3}$). A new side-edge suction force coefficient $\bar{K}_{v,se}$ is derived which in the combination, $\bar{K}_{v,se}\sin^{5/3}\alpha\cos\alpha$, improves the side-edge suction force estimation.

Analytical Formulas

The set of semiempirical formulas[1] correlating the numerical results[2] of the extended Multhopp method is completed by a new side-edge suction force coefficient, $\bar{K}_{v,se}$, and by empirical correction factors, F_1-F_3, introduced in order to obtain correlation with experiments.[2] The domain of application for the empirical approximations is restricted to $M<0.2$-0.3, $|\alpha|<32$ deg, and $A<4$-5, $|\alpha A|<40$-45. The symmetric, aerodynamic coefficients are

$$C_L=K_p\sin\alpha\cos^2\alpha F_1+K_{v,le}\sin^2\alpha\cos\alpha F_1 + \bar{K}_{v,se}\sin^{5/3}\alpha\cos\alpha+F_2\cos\alpha \tag{1}$$

$$C_D=C_{D_0}+\Delta C_D=C_{D_0}+C_L\tan\alpha \tag{2}$$

$$C_m=K_p\sin\alpha\cos\alpha F_1(\xi_{ref}-\xi_p-F_3) + K_{v,le}\sin^2\alpha F_1(\xi_{ref}-\xi_{v,le}) + (\bar{K}_{v,se}\sin^{5/3}\alpha+F_2)(\xi_{ref}-\xi_{v,se}) \tag{3}$$

The zero-lift drag coefficient C_{D_0} is taken from the experiments.[2] It is understood here that at $\alpha<0$ the factors $\sin^2\alpha$ and $\sin^{8/3}\alpha$ [see Eq. (11)] are treated as $|\sin\alpha|\sin\alpha$ and $|\sin\alpha|\sin^{5/3}\alpha$, respectively.

The K coefficients are given by

$$\beta K_p=\frac{2\pi\beta A}{2+\sqrt{(4/3)(\beta A)^2+4}} \tag{4}$$

$$\beta K_{v,le}=\frac{\pi\beta A}{2+\sqrt{(1/4)(\beta A)^2+4}} \tag{5}$$

$$\bar{K}_{v,se}=\frac{\pi(2A)^{1/3}}{1+A^{4/3}+(4/5)A^{5/3}} \tag{6}$$

and the dimensionless centers of pressure of the respective aerodynamic item are approximated by

$$\xi_p=\frac{1}{4}\frac{A\cos\alpha}{\sqrt{\{1+A/[10+(A/10)^2]\}A^2+\cos^2\alpha}} \tag{7}$$

$$\xi_{v,le}=0 \tag{8}$$

$$\xi_{v,se}=\frac{1}{2}\left(0.4+\sqrt{\frac{A}{1+A}}\right)\cos(\alpha/2) \tag{9}$$

and the reference point is at 25% of the chord, i.e., $\xi_{ref}=0.25$. The empirical correction factors are defined as

$$F_1=\cos^2\left\{\frac{1+A}{14}[(1+3A)\alpha-45]\right\},\ \arg\geq 0 \tag{10}$$

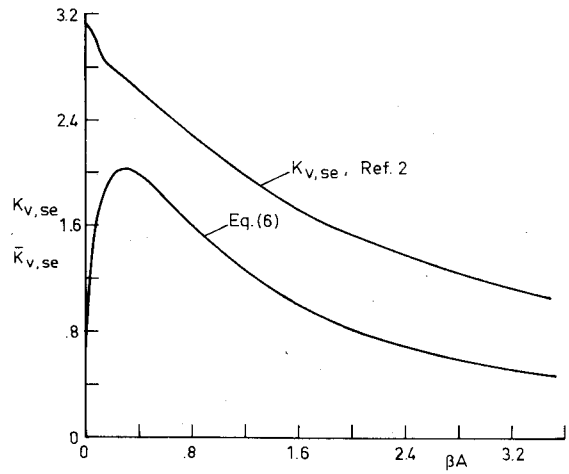

Fig. 1 Side-edge suction force coefficients of rectangular wings as functions of reduced aspect ratio according to different definitions of the angle-of-attack influence; [$K_{v,se}\sin^2\alpha$ from Ref. 2, and $\bar{K}_{v,se}\sin^{5/3}\alpha$ from Eq. (6), respectively].

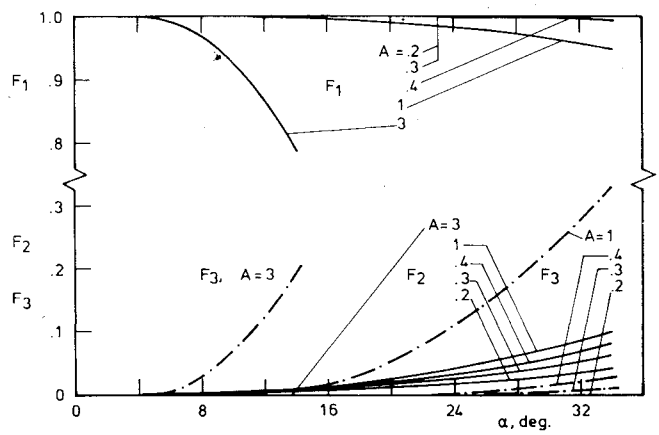

Fig. 2 Empirical correction factors F_1-F_3 [Eqs. (10-12)] as functions of angle of attack and aspect ratio.

$$F_2=\bar{K}_{v,se}\frac{A}{2+A^2}\sin^{8/3}\alpha \tag{11}$$

$$F_3=\sin^2\left\{\frac{12}{(7/2)+A^2}\frac{1+A}{14}[(1+3A)\alpha-45]\right\},\ \arg\geq 0 \tag{12}$$

The first two K coefficients [Eqs. (4) and (5)] are taken from Ref. 1 and the third is a new semiempirically determined coefficient $\bar{K}_{v,se}$ which is combined with $\sin^{5/3}\alpha$ to replace $K_{v,se}\sin^2\alpha$ term derived by Lamar.[2] In Eq. (6) the numerator is taken from Cheng[7] and the denominator is empirical. Equation (6) is shown in Fig. 1 and compared with Ref. 2. Among the alternative curves representing the side-edge suction force coefficient, at most one can be realistic, although necessarily not the correct one. In the present investigation preference is given to curve $\bar{K}_{v,se}$ because it is hard to imagine that the coefficient should not disappear when $A\to 0$. Equations (7-9) are, taken in order: the empirical approximation of the dimensionless center of pressure of the potential flow pressure distribution; the location of the leading-edge suction force; and the length coordinate of the centroid of the side-edge suction force. Equation (7) can be inspected and modified by means of linear theory and by the results of Ref. 8. The approximations of $\xi_{v,le}$ and $\xi_{v,se}$ [Eqs. (8) and (9)] could be inspected and improved by a workable viscous flow theory, where the quantities in question will,

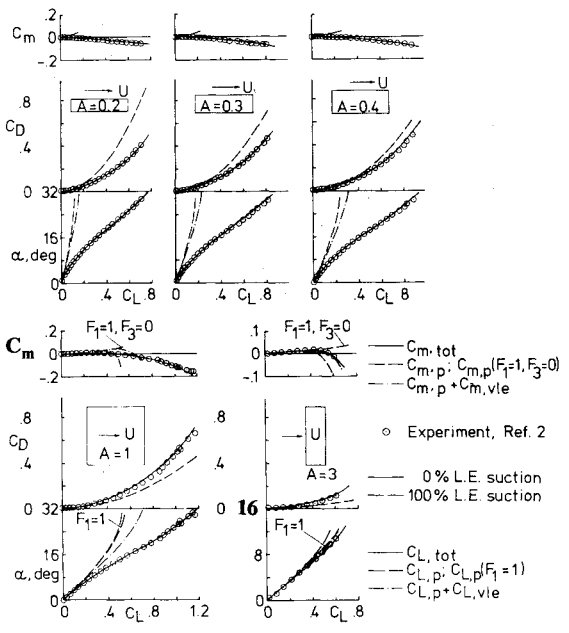

Fig. 3 $C_L(\alpha)$, $C_D(C_L)$, and $C_m(C_L)$ on sharp-edged rectangular wings of aspect ratios $A=0.2$, 0.3, 0.4, 1, and 3 at $M=0.2$ [experiments according to Ref. 2 compared with present semiempirical formulas, Eqs. (1-12)].

however, be implicitly hidden. A small positive quantity would most probably be a better approximation of $\xi_{v,le}$ than Eq. (8).

The empirical F factors [Eqs. (10-12)] are subjective compositions with the only merits of being simple and fulfilling their intended tasks, namely: to correct for the losses in potential lift [F_1] due to losses in circulation; to correct for the corresponding wandering of the center of pressure of the potential flow pressure distribution [F_3]; and to give a higher order correction term [F_2] to the side-edge suction force coefficient $\bar{K}_{v,se}$ at high angles of attack. The factor F_2 could be recognized as the contribution from the secondary vortices and can be neglected for $\alpha < 10$-15 deg. The correction factors are plotted in Fig. 2, where it can be seen that for $A \leq -0.4$, F_1 is negligible in the actual angle-of-attack interval, $\alpha < |32|$ deg, and that F_3 can be neglected for $\alpha < |25|$ deg. As A increases from $A=0.4$, F_1 first decreases quite slowly for increasing α up to $A=1$, and thereafter decreases faster with increasing A. The factor F_3 shows a corresponding but opposite trend for increasing A with a rapid increase from $A=0.4$.

Results

The numerical results are compared with experiments[2] at the subsonic Mach number, $M=0.2$, on sharp-edged rectangular wings having the aspect ratios $A=0.2$, 0.3, 0.4, 1, and 3. Evaluating the set of Eqs. (1-12) and observing that the arguments of the correction factors F_1 and F_3 [Eqs. (10) and (12)] are not allowed to take a negative sign, the solid-line curves in Fig. 3 are obtained for the total coefficients. Curves for the attached flow (potential flow) characteristics and for the sum of potential flow and leading-edge separated flow characteristics are also shown. The potential flow curves with $F_1=1, F_3=0$ completely cover Lamar's[2] potential flow result. The correlation between the set of equations [Eqs. (1-12)] and experiments is, from an engineering point of view, quite satisfactory.

Conclusions

Improved correlation with experiments in incompressible flow, up to moderately high angles of attack (depending on the aspect ratio), is obtained by using an $\alpha^{5/3}$ dependence of the side-edge singularity of sharp-edged rectangular wings.

Empirical correction factors have been developed which make it possible to obtain good correlation with experimental results on sharp-edged rectangular wings up to high angles of attack, where flow separation effects have already built up.

Acknowledgment

This work has been supported by the Materiel Administration of the Armed Forces, Air Materiel Department, Missiles Directorate, Sweden.

References

[1] Larson, E.S., "Sharp-Edged Rectangular Wing Characteristics," *Journal of Aircraft*, Vol. 18, Oct. 1981, pp. 895-896.

[2] Lamar, J.E., "Extension of Leading-Edge Suction Analogy to Wings with Separated Flow Around the Side Edges at Subsonic Speeds," NASA TR R-428, Oct. 1974.

[3] Polhamus, E.C., "A Concept of the Vortex Lift of Sharp-Edge Delta Wings Based on a Leading-Edge-Suction Analogy," NASA TN D-3767, Dec. 1966.

[4] Kaden, H., "Aufwicklung einer unstabilen Unstetigkeitsfläche," *Inqenievr-Archiv*, II Band, Mai 1931, pp. 140-168.

[5] Legendre, R., "Ecoulement au voisinage de la pointe avant d'une aile a forte fleche aux incidences moyennes," *La Recherche Aéronautique*, No. 30, Nov./Dec. 1952, pp. 3-8; No. 31, Jan./Feb. 1953, pp. 3-6; No. 35, Sept./Oct. 1953, pp. 7-8.

[6] Adams, M.C., "Leading-Edge Separation from Delta Wings at Supersonic Speeds," *Journal of Aeronautical Sciences*, Vol. 20, June 1953, p. 430.

[7] Cheng, H.K., "Remarks on Nonlinear Lift and Vortex Separation," *Journal of Aeronautical Sciences*, Vol. 21, March 1954, pp. 212-214.

[8] Holme, O.A.M., "Measurements of the Pressure Distribution on Rectangular Wings of Different Aspect Ratios," FFA Meddel. Rept. 1950.

AIAA 81-2368R

Advanced-Range Instrumentation Aircraft Improvement and Modernization Program

James S. Nash*
Wright-Patterson Air Force Base, Ohio

Background

THE advanced-range instrumentation aircraft (ARIA) are seven EC-135 aircraft equipped with telemetry acquisition systems and are used to support: 1) satellite launches from Cape Canaveral Air Force Station, Fla., and Vandenberg Air Force Base, Calif.; 2) telemetry coverage of instrumented re-entry vehicles in the terminal area during ballistic missile testing; and 3) telemetry relay and command/destruct capabilities during air-launched cruise missile testing.

Exterior modifications to the C-135 airframe were required to provide the telemetry support capability. These modifications include the addition of a 7 ft dish antenna to the aircraft nose, two high-frequency (HF) wing probe antennas, a 125 ft HF trailing wire antenna, three ultrahigh-

Presented as Paper 81-2368 at the AIAA/SETP/SFTE/SAE/ITEA/IEEE 1st Flight Testing Conference, Las Vegas, Nev., Nov. 11-13, 1981; submitted Nov. 16, 1981; revision received Feb. 8, 1982. This paper is declared a work of the U.S. Government and therefore is in the public domain.

*Chief, Systems Engineering Branch, 4950th Test Wing.